

# Orange juice facilitated eco-friendly synthesis of visible light active ZnFe<sub>2</sub>O<sub>4</sub> nanoparticles and its photocatalytic applications

S.B. Patil,<sup>1,2\*</sup> G. Nagaraju,<sup>2</sup> H.S. Bhojya Naik<sup>3</sup>

<sup>1</sup>Department of Chemistry, The oxford college of science, Bengaluru,560102,India

<sup>2</sup>Department of Chemistry, Siddaganga institute of technology, Tumakuru-572103, India

<sup>3</sup>Department of Studies and Research in Industrial Chemistry, School of Chemical, Sciences, Kuvempu University, Shankaragatta-577451, India

**Abstract:** Herein, the ZnFe<sub>2</sub>O<sub>4</sub> nanoparticles were synthesized by cost effective and eco-friendly orange juice assisted combustion method at 500 °C for 10 minutes. Characterized by different Spectro photochemical techniques, such as X-ray diffraction (XRD), that confirms the formation of cubic structure with space group Fd3m, Fourier transform infrared spectra (FTIR) shows the metal-Oxygen bonding, Ultraviolet-visible absorbance spectra confirms the absorbance peak at visible light around 300-400 nm, from scanning electron microscopy (SEM) observed the agglomerated, irregular shaped nanoparticles. In the presence of ZnFe<sub>2</sub>O<sub>4</sub> nanoparticles, the percentage of rose bengal dye degradation is reached 96 % within 150 minutes under visible light region in acidic medium. This work can be influencing the ZnFe<sub>2</sub>O<sub>4</sub> nanoparticles can acts as a good visible active catalyst in waste water effluent treatment.

**Keywords;** Photocatalyst, Dye degradation, Ferrites, Visible light, Rose bengal

## INTRODUCTION

The growth of environmentally caring photocatalyst is of significance in the present era. The most dynamic feature of a photocatalyst for its industrial waste effluent treatment is its ability to be well reused and recovered after the photocatalytic reaction process. Several physical and chemical methods such as filtration, centrifugation and chromatography, etc. are tedious and also affect a lot of problems [1-2]. The advanced oxidation method using magnetically separable nano sized photocatalyst is emerging to be a robust in removal of dye molecules from waste effluent [3]. Subsequently the sustainability of magnetic photocatalyst fulfills the principles of green chemistry. The degradation of textile effluents by photocatalytic process in the presence of semiconductor photocatalysts has the effect to be a beneficial method for water effluent treatment [4].

\* patilSB862@gmail.com

For the past decades, metal oxide nanomaterials such as TiO<sub>2</sub>, BiWO<sub>4</sub>, MnO<sub>2</sub>, Fe<sub>2</sub>O<sub>3</sub>, ZnO etc., have been synthesized due to their unique chemical and physical properties; penetrating research has been carried out in photodegradation reaction [5-6]. ZF nanoparticles have fascinated consideration owing to their magnetic property and advanced applications as compared to its bulk. This nanoparticle can be removed from the reaction mixture by applying some magnetic field. It is a good semiconductor and exhibited low optical energy band gap of 2.2 eV hence it establishes the more electron-hole recombination system in the presence of visible light. ZF has been widely used in the degradation of organic molecules via catalytic reactions under different light irradiations [7]. Several methods involved in the synthesis of ZF nanoparticles like co-precipitation method, sol-gel method, hydrothermal

methods, combustion methods, etc., [8-9] In this article ZF nanoparticles were synthesized using eco-friendly and cost-effective combustion method by taking a different volume of orange juice, it acts as a combustion fuel. In this method orange juice composed of citric acid, it acts a reducing agent and the nitrate salts acts as an oxidizing agent. Synthesized nanoparticles were calcinated at higher temperature and used to degrade the organic dyes. Here RB dye used as a model pollutant to check the catalytic activity of ZF nanoparticles under visible light.

## METHODS

### Chemicals required

The analytical grade of chemicals such as ferric nitrate nonahydrate [ $\text{Fe}(\text{NO}_3)_3 \cdot 9\text{H}_2\text{O}$ , 99%], Zinc nitrate tetrahydrate [ $\text{Zn}(\text{NO}_3)_2 \cdot 6\text{H}_2\text{O}$ , 99%] were purchased from SD fine chem. limited. Orange juice purchased during February-2019 from natural juice centre Shankaragatta, Shimoga, Karnataka. 0.1 N NaOH and dil. HCl used to maintain the pH of the dye solution.

### Synthesis of $\text{ZnFe}_2\text{O}_4$ nanoparticles

The  $\text{ZnFe}_2\text{O}_4$  nanoparticles were synthesized by green combustion method using orange juice as a fuel. In 2.5 mL of orange juice dissolved the 2:1 stoichiometric molar ratio of  $\text{Fe}(\text{NO}_3)_3 \cdot 9\text{H}_2\text{O}$  and  $\text{Zn}(\text{NO}_3)_2 \cdot 6\text{H}_2\text{O}$ . This solution was kept in a muffle furnace at 500 °C for 10 minutes, then product was obtained. The above experiment was repeated by taking the volume of juice as 5 mL, 7.5 mL and 10 mL and named it as ZnFe-2.5 mL, ZnFe-5 mL, ZnFe-7.5 mL, ZnFe-10 mL. All these obtained products were calcinated in muffle furnace at 600 °C about 4 h. Then calcinated nanoparticles were used for further characterization and their application given below.

## RESULTS AND DISCUSSION

Fig 1 shows the XRD spectrum of all synthesized nanoparticles. The crystallite size of the Nps were identified by Philips X-pert pro

prefix powder X-ray diffractometer with  $\text{CuK}\alpha$  radiation. The position of two theta and intensity of all the diffraction peaks were well assigned to the formation of spinel structure with cubic space and space group  $\text{Fd}3\text{m}$ . The peaks could be indexed in the figure, which are well matched with JCPDS file (card no. 86-2267)

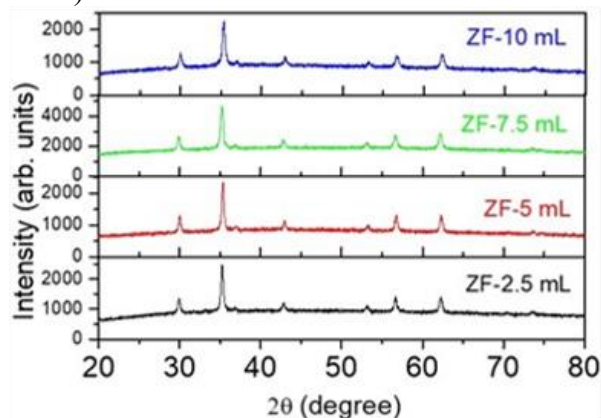


Figure 1. XRD patterns of ZF nanoparticles synthesized by combustion method

[10]. The average crystallite size of all samples was calculated by the following Debye–Scherrer equation 1. The crystallite size of ZF-2.5 mL, ZF-5 mL, ZF-7.5 mL, ZF-10 mL nanoparticles found to be 28 nm, 26 nm, 24 nm and 27 nm respectively.

$$D = 0.89\lambda/\beta\cos\theta \dots \dots \dots \text{eq. (1)}$$

Here, D represents the crystallite size of the nanoparticles,  $\lambda$  is the wavelength of X-ray (1.54 Å) used,  $\beta$  is fullwidth at half maxima, and  $\theta$  will be the diffraction angle.

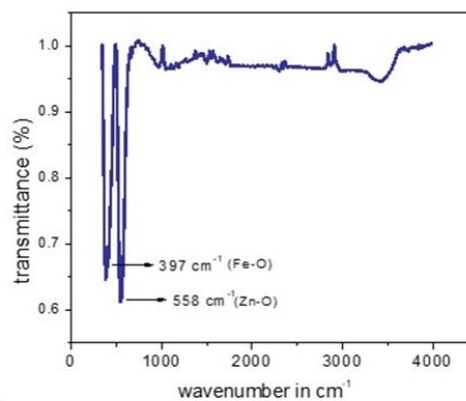


Figure 2. FTIR spectrum of ZF-2.5 mL nanoparticles.

The Fig. 2 represents the FTIR spectrum of ZF-7.5 mL nanoparticles between the ranges of 350-4000  $\text{cm}^{-1}$ . This spectrum shows two strong absorption peaks at below 600  $\text{cm}^{-1}$ , reason is that the vibration of oxygen atom with highest valence metal cations in ferrites. [11]. In which, between (374-390)  $\text{cm}^{-1}$  peak assigned to the characteristic of intrinsic stretching mode of Fe-O bond at octahedral site and (548-550)  $\text{cm}^{-1}$  peak corresponds to the vibrational mode of Zn-O bond at tetrahedral site of spinel ZF-7.5 mL nanoparticles. The broad peaks at 3432  $\text{cm}^{-1}$  and 1109  $\text{cm}^{-1}$  arise due to the formation of O-H and C-O stretching bond, respectively.

Fig. 3(a) represents the SEM image of ZF-7.5 mL nanoparticles. The micrograph shows both enlarge and tiny spherical structure. The morphology represents the agglomerated nanoparticles because of its magnetic nature, the particles are get attracted each other. Fig.3(b) demonstrated the EDAX analysis of ZF-2.5 mL nanoparticles. It was carried out to identify its elemental composition. From this spectrum confirmed that the presence of Fe, Zn and O elements. Along with those atoms, a small percentage of Carbon also observed.

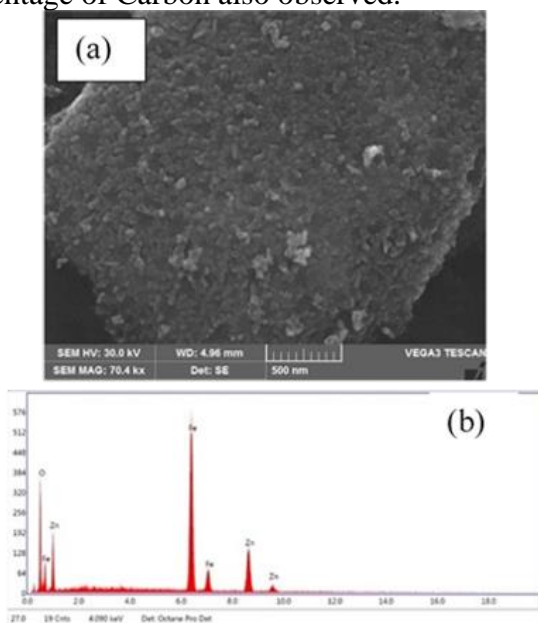


Figure 3. (a) SEM with (b) EDAX spectrum of ZF-2.5 mL nanoparticles.

The UV-visible absorption spectrophotometer is a powerful technique to identify the optical properties of semiconductor nanoparticles. The absorbance of nanoparticles in UV-visible absorption spectra depends on the following factors i.e., oxygen deficiency, crystallite size, surface morphology and property of substituting materials [12]. Fig. 4 shows the strong absorbance spectra of  $\text{ZnFe}_2\text{O}_4$  nanoparticles. The absorbance peak shifts towards higher wavelength (red shift) along with increasing volume of orange juice, beyond 7.5 mL the blue shift observed. It revealed that ZF-7.5 mL nanoparticles absorb more visible light and helps more in the degradation of organic molecules.

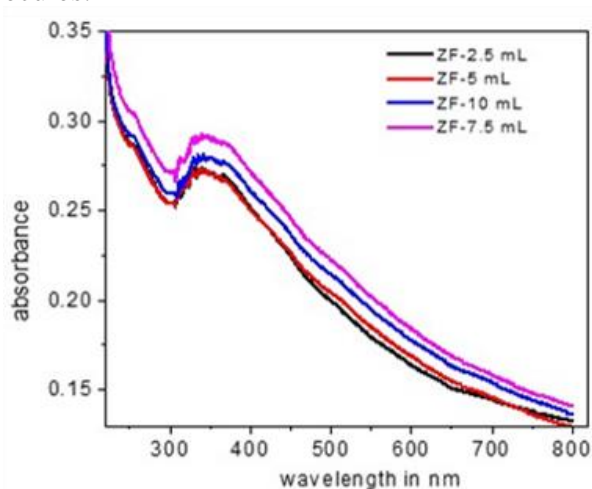


Figure 4 UV-visible absorption spectra of ZF nanoparticles.

The photodegradation of RB dye was taken in the presence of ZF-7.5 mL nanoparticles under visible light source. In photodegradation process, 30 mg of ZF-7.5 mL nanoparticles were added into 100 mL of RB dye solution with a concentration of 5 ppm. Before irradiation under visible light, the reaction solution was stirred well in the dark condition about 1 hour to maintain adsorption-desorption equilibrium. After that the solution was irradiated under visible light irradiation, continuous stirring was maintained to allow the solution in suspension. At 30 minutes of time interval, supernatant solution was taken from the RB solution until

the RB colour was disappeared and then magnetically separated in order to remove the nanoparticles catalyst can be reused for further photodegradation runs. The absorbance of the collected samples was monitored at 543 wavelength maximum on Ultra violet visible absorption spectrophotometer in the range of 200-800 nm.

Fig. 5. shows the UV-visible absorbance spectra of photodegraded RB dye solution. Here, we are observing the decreasing the intensity of absorbance peak at 543 nm as irradiation of visible light increases. The reason is that as the time of visible light irradiations increases the decomposition of organic molecules also increases [13]. The mechanism involved is that due to the lower energy band gap of ZF-7.5 mL, the number of electrons excited from valence band to conduction band increases with increasing a greater number of holes in valence band. The photoinduced holes react with RB or interact with hydroxyl ions to generate more hydroxyl radicles, which are strong oxidant for the decomposition of organic molecules. Hence, hydroxyl radicals, hydroxyl ions, electrons and hole could involve in the breaking of organic dyes [14-15].

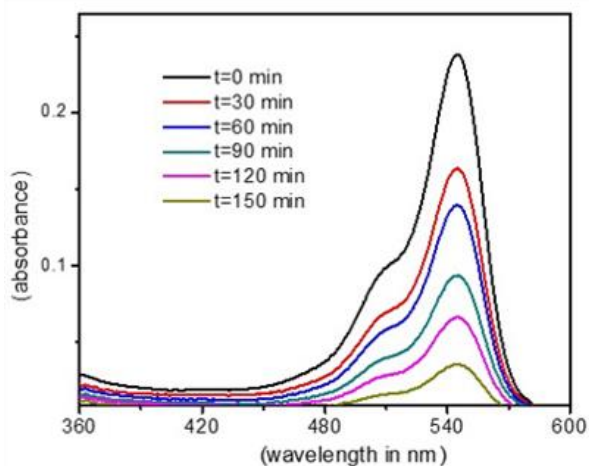


Figure 5. UV-visible absorbance spectra of RB during degradation.

Percentage of photocatalytic degradation for organic dyes is calculated by equation (2).

$$\% \text{ of degradation} = [(C_0 - C_t) / C_0] \times 100 \dots \text{Eq. (2)}$$

Where,  $C_0$  is the initial absorbance of RB dye solution;  $C_t$  is the absorbance of RB dye solution at certain time intervals of degradation process.

The percentage degradation of RB dye is shown in Fig.6. Here we observed that in dark

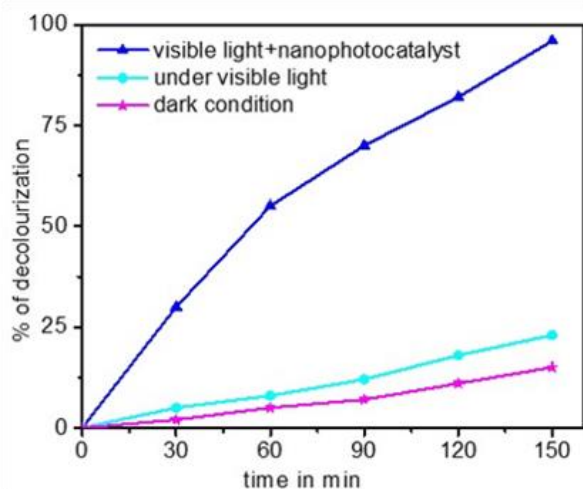


Figure 6. Percentage degradation of RB dye in the presence of ZF-2.5 mL nanoparticles

condition the percentage of absorption of RB over ZF nanoparticles was reached to 10 %. In the absence of catalyst, the RB dye solution was irradiated under visible light, only 24 % of dye degraded within 150 minutes. But in the presence of ZF nanocatalyst, it was reached to 96 % within 150 minutes.

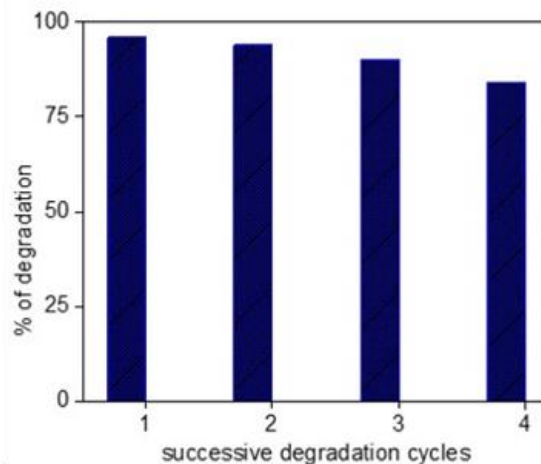


Figure 7. Reusability of ZF-2.5 mL nanoparticles over four successive photodegradation cycles.

The reusability and stability of the photocatalyst is an important measure in long term use it as a photocatalyst in photodegradation. To evaluate stability and reusability, the recycled ZF nanoparticles were subjected to next four cycles of degradation process with the same concentration of RB dye under visible light radiation. After each cycle the nanocatalyst was separated by applying magnetic field and washed with distilled water and ethanol then dried in an oven about 3h to get rid of adsorbed RB dye on the surface of nanocatalyst. The percentage degradation of RB over four degradation cycles was carried out, its result is shown in the Fig.7. From the result, the catalytic activity of the ZF nanoparticles was decreased by 15 % even after the 4<sup>th</sup> cycle. It revealed that ZF nanoparticles makes notable catalyst in dye degradation.

## CONCLUSION

In this work ZF nanoparticles were synthesized by simple combustion method using orange juice. XRD confirmed the formation of cubic spinel structure, FTIR confirms the presence of characteristic of Zn-O and Fe-O vibration modes. These nanoparticles absorb the visible light that responsible for the degradation of organic dyes. The photodegradation of RB is reached to 96 % under visible light irradiations. The reusability showed the stability of ZF nanoparticles towards dye degradation. This work implies that ZF could be used as a visible nanocatalyst in textile effluent treatment.

## ACKNOWLEDGMENT

One of the authors Dr. G. Nagaraju thanks DST-SERB (SB/FT/CS-083/2012) Govt of India, New Delhi for providing characterization techniques. And also authors thank Siddaganga institute of technology, Tumakuru, Karnataka, India and Kuvempu university, Shimoga, Karnataka, India for providing lab facilities to carry out this research work.

## ABBREVIATIONS

ZF Zinc ferrite, RB rose Bengal

## REFERENCES

1. F. Martinez, J.A. Melero, J.A. Botas, M.I. Pariente, R. Molina, Treatment of phenolic effluents by catalytic wet hydrogen peroxide oxidation over Fe<sub>2</sub>O<sub>3</sub>/SBA-15 extruded catalyst in a fixed-bed reactor, *Ind. Eng. Chem. Res.* **46**, 4396-4405 (2007).
2. K. Simeonidis, S. Mourdikoudis, E. Kaprara, M. Mitrakas, L. Polavarapu, Inorganic engineered nanoparticles in drinking water treatment: a critical review, *Environ. Sci. Water Res. Technol.* **2**, 43 (2016).
3. K.N. Harish, H.S. Bhojya Naik, P.N. Prashanth kumar, R. Viswanath, Synthesis, enhanced optical and photocatalytic study of CdZn ferrites under sunlight, *Catal Sci Technol* **2**, 1033-1039 (2012).
4. S.B. Patil, Shivaraj B. Patil, G Nagaraju, A.V. Raghu A.V, K. Raghava Reddy, Review article: Recent progress in metal-doped TiO<sub>2</sub>, non-metal doped/codoped TiO<sub>2</sub> and TiO<sub>2</sub> nanostructured hybrids for enhanced photocatalysis. *International journal of hydrogen generation.* **45**, 7764-7778 (2020)
5. Udayabhanu, G. Nagaraju, H. Nagabhushana, D. Suresh, C. Anupama, G.K. Raghu, S.C. Sharma, Vitis labruska skin extract assisted green synthesis of ZnO super structures for multifunctional applications, *Ceram. Int.* **5** 351 (2017).
6. S.K. Jesudoss, J. Judith Vijaya, L. John Kennedy, P.I. Rajan, Hamad A. Al-Lohedan, R.J. Ramalingam, K. Kaviyarasu, M. Bououdina, *J. Photochem. Photobiol. B* **165**, 121 (2016).
7. S.B. Patil, H.S. Bhojya Naik, G. Nagaraju, R. Viswanath, S.K. Rashmi, M. Vijay kumar, Sugarcane juice mediated eco-friendly synthesis of visible light active zinc ferrite nanoparticles: Application to degradation of mixed dyes and antibacterial activities *Mater. Chem. Phys.* **212**, 351 (2018).

8. S.E. Shrirath, M.L. Mane, Y. Yasukawa, X. Liua, A. Morisako, *Phys. Chem. Chem. Phys.* **16**, 2347 (2014).
9. S. Ayyappan, G. Paneerselvam, M.P. Antony, J. Philip, Structural stability of ZnFe<sub>2</sub>O<sub>4</sub> nanoparticles under different annealing conditions, *Mater. Chem. Phys.* **128**, 400-404 (2011).
10. S.B. Patil, H.S. Bhojya Naik, G. Nagaraju, R. Viswanath, S.K. Rashmi, Synthesis of visible light active Gd<sup>3+</sup> substituted ZnFe<sub>2</sub>O<sub>4</sub> nanoparticles for photocatalytic and antibacterial activities, *Eur. Phys. J. Plus* **132**, 328 (2017).
11. X. Li, Y. Hou, Q. Zhao, L. Wang, A general, one-step and template-free synthesis of sphere-like zinc ferrite nanostructures with enhanced photocatalytic activity for dye degradation, *J. Colloid. Interface Sci.* **358** 102-108 (2011).
12. K.N. Harish, H.S. Bhojya Naik, P.N. Prashanth kumar, R. Viswanath, Optical and Photocatalytic Properties of Solar Light Active Nd-Substituted Ni Ferrite Catalysts: For Environmental Protection *ACS Sustain. Chem. Eng.* **1**, 1143 (2013).
13. F. Martinez, J.A. Melero, J.A. Botas, M.I. Pariente, R. Molina, Treatment of phenolic effluents by catalytic wet hydrogen peroxide oxidation over Fe<sub>2</sub>O<sub>3</sub>/SBA-15 extruded catalyst in a fixed-bed reactor, *Ind. Eng. Chem. Res.* **46**, 4396-4405 (2007).
14. S. Sun, X. Yang, Y. Zhang, F. Zhang, J. Ding, J. Bao, C. Gao, Enhanced photocatalytic activity of sponge-like ZnFe<sub>2</sub>O<sub>4</sub> synthesized by solution combustion method, *Prog. Nat. Sci.: Mater. Int.* **22 (6)** 639-643 (2012).
15. Patil S. B, Bhojya Naik H. S, Nagaraju G, Kumaraswamy B. E, Raghava Reddy K, Enhanced Photocatalytic Activity and Biosensing of Gadolinium Substituted BiFeO<sub>3</sub> Nanoparticles, *Chemistry Select*, **3**, 9025–9033 (2018)